

Journal of Materials Chemistry B

Accepted Manuscript



This is an *Accepted Manuscript*, which has been through the Royal Society of Chemistry peer review process and has been accepted for publication.

Accepted Manuscripts are published online shortly after acceptance, before technical editing, formatting and proof reading. Using this free service, authors can make their results available to the community, in citable form, before we publish the edited article. We will replace this *Accepted Manuscript* with the edited and formatted *Advance Article* as soon as it is available.

You can find more information about *Accepted Manuscripts* in the [Information for Authors](#).

Please note that technical editing may introduce minor changes to the text and/or graphics, which may alter content. The journal's standard [Terms & Conditions](#) and the [Ethical guidelines](#) still apply. In no event shall the Royal Society of Chemistry be held responsible for any errors or omissions in this *Accepted Manuscript* or any consequences arising from the use of any information it contains.



Potential of PVA-doped bacterial nano-cellulose tubular composites for artificial blood vessels

Jingyu Tang,^a Luhan Bao,^a Xue Li,^a Lin Chen^a and Feng F. Hong^{*a,b}

Received 13th June 2015,
Accepted XXth XX 2015

DOI: 10.1039/x0xx00000x

www.rsc.org/

Bacterial nano-cellulose (BNC) hydrogel has been suggested to be a promising biomaterial for artificial blood vessel. However, some properties of BNC do not reach all the requirement of a native blood vessel, for instance compliance. In order to improve the properties of BNC tubes, poly(vinyl alcohol) (PVA) was introduced in the BNC tubes to make composites. Two types of pristine BNC tubes with different inner structures were produced in two bioreactors. A PVA tube and PVA-BNC tubular composites were made for comparison by using a thermally-induced phase separation method. The morphology, water permeability, cytotoxicity, as well as mechanical properties including axial stretch strength, suture retention, burst pressure, and compliance of all the tubes were evaluated and compared. The results indicated that PVA impregnated into BNC tubes and then significantly improved the properties of BNC, especially the mechanical properties and water permeability. BNC tube itself played great effects on the performances of the composites as the skeleton base material. The PVA-BNC composite tubes would provide new biomaterial candidates for vascular grafts.

Introduction

Vessel transplantation is the main treatment for vascular disease that is one of the most common diseases causing great challenge to human health¹. Most of surgical procedures associated with blood vessels are in small-caliber (<6 mm) vessels². Although some artificial blood vessels (e.g. Dacron and ePTFE) have been used successfully in clinic for large-caliber vessels, the performances of these materials on small-caliber vessels are poor^{3,4}. Development of new materials suitable for the replacement of small blood vessels is still under way.

Bacterial nano-cellulose (BNC) formed by repeated dimers of β-1,4 linked D-glucose units has been reported to perform some unique properties, including high chemical purity, ultrafine nano-fiber network, high crystallinity, high water holding capacity, excellent wet tensile strength, and good biocompatibility^{5,6}. It has been certified to be a promising biomedical material, which can be widely used in wound dressing, artificial skin, bone tissue scaffold and arterial stent coating⁷⁻⁹. BNC tubes have also been reported to have great potential for blood vessel replacement^{10,11}. The nanofibers provide support for the attachment and proliferation of cells¹⁰. And the unique network structure may work like the collagen network of the extracellular matrix for the transmission of nutrition and metabolites¹⁰. Animal experiments in mice and pigs have showed admirable patency and fine epithelialization in the internal surface of the tubes^{4,12}.

BNC tubes are usually prepared via *in situ* fermentation in various cultivation devices. Basically, there are four kinds of cultivation devices applied in BNC tubes preparation, three of which have been reviewed by Hong et al.¹³. Briefly, the first kind of device consists of a vertically placed tubular glass vessel, whose centre is fixed a glass stick or tube. A small BNC tube with short length can be obtained at the interface of air and the culture medium between the gaps in the device when an inoculated culture medium is filled in and statically incubated for 7–14 days. The second device is constructed by fixing an oxygen-permeable silicone tube with an oxygen in-flow in a culture medium. A BNC tube forms on the outside surface of the silicone tube after static cultivation for several days. The third device is composed with a glass rod fixed horizontally in the core of a tubular culture vessel consisting of two half-pipes. The device is placed on the surface of a precultured BNC pellicle. During the continued-cultivation, the newly generated nanocellulose will grow into the culture vessel through the gaps between the two half-pipes to form a BNC tube. The BNC tubes prepared in the above three types of devices all shows a multilayered structure, which may cause danger in long term application. Therefore Hong et al. designed the fourth device, a double-silicone-tube bioreactor, by fixing a small silicone tube in the centre of a bigger silicone tube. The whole device is placed in an oxygen container. Both silicone tubes can supply oxygen to the culture medium and BNC tube forms efficiently in the device. Interestingly, the finally obtained BNC tube demonstrates a non-layered structure and enhanced properties¹³⁻¹⁵. Although the BNC tubes perform some good mechanical properties, the poor elasticity of BNC would restrict the application of BNC tubes as vascular grafts. This is because lumen occlusion is usually caused by compliance mismatch between the graft and the native vessel^{16,17}.

^a Group of Microbiological Engineering and Industrial Biotechnology, College of Chemistry, Chemical Engineering and Biotechnology, Donghua University, North Ren Min Road 2999, Shanghai 201620, PR China. E-mail: fhong@dhu.edu.cn

^b Key Laboratory of High Performance Fibers & Products, Ministry of Education, Donghua University, Shanghai 201620, PR China.

See DOI: 10.1039/x0xx00000x

Poly(vinyl alcohol) (PVA) can be easily made into elastic hydrogel by chemical crosslinking or physical crosslinking, for example a low temperature thermal cycling process¹⁸⁻²¹. It has been reported to composite with BNC to improve mechanical, biocompatible and other performances. Gea et al. prepared BNC/PVA bio-nanocomposites by addition of PVA into the inoculated culture medium during an *in situ* cultivation²². The addition of PVA weakens the interaction of hydrogen-bonds between the BNC molecules, which improves the toughness. However, only small amount of PVA can combine with BNC fibers after the purification process. Methods such as casting-drying²³⁻²⁵, electron beam or γ -irradiation cross-linking²⁶ and chemical cross-linking²⁷ are usually applied to prepare dry BNC/PVA composite membranes with improved properties for applications of package materials^{23,24,26} or drug controlled release²⁵. Physical cross-linking method using thermal cycling is widely used in preparation of BNC/PVA composite hydrogels for biomedical engineering applications as a reason for non residual of toxic chemical cross-linking reagents²⁸⁻³⁰. Moreover, the mechanical properties of the BNC/PVA composites can be modified by regulating the freezing temperature and holding time, thawing rate and number of freeze/thaw cycles.

Some of these composites perform anisotropic mechanical properties and good hemocompatibility, which are important for blood vessel replacement^{31,32}. Unlike ePTFE, nanocomposite of BNC impregnated with PVA performs low activation of Factor XII and platelets³². Reduction of the total number of free surface-OH groups in both PVA and BNC may cancel out the complement system activation³². To our knowledge, tubular BNC/PVA composites were rarely reported. Millon et al. produced the BNC/PVA nanocomposite tubes with anisotropic mechanical properties by adding PVA powder to aqueous suspensions of BNC, which was obtained via shaking culture²⁹. However, this kind of composite can not demonstrate the intact nano-fibril network and unique properties from the BNC tubes that are obtained via static cultivations. It has not been reported yet that the PVA-BNC composite tubes can be produced by doping PVA into statically-cultured BNC tubes to maintain the innate intact structure of BNC tubes.

In this study, PVA-doped BNC composite tubes were produced from the innate BNC tubes that formed in static cultivations, and were evaluated in comparison with the BNC tubes for the potential in artificial blood vessel. Two kinds of BNC tubes with different structures were produced in two bioreactors. Hydrogel-like BNC/PVA composite tubes were made based on the two BNC tubes via thermally induced phase separation method. This technique retained the unique network of BNC tubes. PVA penetrated into the space of BNC fibers to form composite hydrogel. The mechanical properties including axle stretch strength, burst pressure, suture retention, circumferential dynamic compliance of BNC tubes, PVA tubes and BNC/PVA composite tubes were compared. The morphology, water permeability and cytotoxicity were studied as well. The results showed that this new tubular composite material may be a promising candidate for blood vessel replacement.

Results and discussion

Morphology

Fig. 1 illustrates the macro-morphology of BNC tubes, PVA tube and BNC/PVA composite tubes. For BNC tubes, the D-BNC tube possesses bigger external diameter and more homogeneous character along the diametric direction than the S-BNC tube. The S-BNC tube possesses denser nano-cellulose close to the inner wall, which may weaken the transmission of light illustrated in Fig. 1. However, the nano-cellulose becomes looser at the area near the external wall. The PVA tube is less transparent than the BNC tubes. As a result, both S-BNC/PVA and D-BNC/PVA composite tubes are less diaphanous. As the PVA tube and the BNC/PVA composite tubes were all prepared in the same mould, they all perform good homogeneity at both axle and circumferential directions.

Fig. 1 Macro-morphology of S-BNC tube (a), D-BNC tube (b), S-BNC/PVA composite tube (c), D-BNC/PVA composite tube (d) and PVA tube (e).

From the SEM images illustrated in Fig. 2, both S-BNC and D-BNC tubes are all fabricated by nano-fiber network. For S-BNC tube, fibers at the inner side of the tube wall are thicker than the fibers at the outside of the tube wall (Fig. 2a and 2b). Fig. 2C shows that a multilayered structure can be observed on the cross section, as same as described previously in other groups³³. For the single silicone tube bioreactor, bacterial cells should first gathered around the silicone tube, which can be regarded as the gas-liquid interface, and began to secrete nano-cellulose to form a thin BNC tube, according to the cellulose synthetic mechanism^{5,11}. The BNC around the silicone tube may impede the diffusion of oxygen to farther distance. So more bacterial cells gathered to the silicone tube and more cellulose was produced to probably form fibers with wider diameter. In a similar way, fibers at the inner side and external side of D-BNC tube made by the double silicone tubes thereafter had similar diameter, since oxygen diffused from both the inner silicone tube and the outside silicone tube. Our previous work has already showed that bacterial cells are able to secrete BNC at both interfaces simultaneously¹³. As a result, two separate BNC films grow together to form an intact BNC tube. Fig. 2F shows that there is no layered structure on the cross section of D-BNC tube but looser nano-fiber network, similarly as reported previously¹³.

Fig. 2 SEM micrographs and fiber diameter distributions of BNC tubes. SEM images of external surface (A), internal surface (B), and cross section (C) of S-BNC tube, as well as distribution of fiber diameter corresponding to image A (a), B (b), and C (c), are shown respectively. SEM image of external surface (D), internal surface (E), and cross section (F) of D-BNC tube, as well as distribution of fiber diameter corresponding to image D (d), E (e), and F (f), are shown respectively.

Fig. 3 shows the internal side and outside morphology of PVA tube and BNC/PVA composite tubes. For PVA tube, porous structure like sponge can be found at the outside surface (Fig. 3C and 3c). The internal surface possesses less porous and much denser structure (Fig. 3F and 3f). The structure difference may be caused by heterogeneous phase separation along the diametric direction of

the tube. Image of internal side of S-BNC/PVA composite tube illustrates many nano-fibers and small pores (Fig. 3d). It can be found that PVA penetrated into the space between the fibers to form entangled structure with some BNC fibers (Fig. 3D and 3d). The outside morphology of S-BNC/PVA composite tube is similar as that of PVA tube (Fig. 3A and 3a). The nanofiber network at the inner side of S-BNC/PVA composite tube and the porous structure at the external surface may provide an interesting graft for endothelialization of the luminal surface and tissue regeneration by smooth muscle cells growth from the external surface. For D-BNC/PVA composite tube, the outside morphology (Fig. 3B) is homogeneous with the internal side morphology (Fig. 3E).

Fig. 3 SEM micrographs of: S-BNC/PVA composite tube, D-BNC/PVA composite tube and PVA tube. The external surfaces of S-BNC/PVA composite tube (A), D-BNC/PVA composite tube (B) and PVA tube (C), as well as the internal surfaces of S-BNC/PVA composite tube (D), D-BNC/PVA composite tube (E), and PVA tube (F) are displayed in amplification of 1000 times, respectively. SEM images of a-f in amplification of 5000 times correspond to the images of A-F.

Size and component analysis

Tab. 1 illustrates the wall thickness of S-BNC tube was about 0.65 ± 0.11 mm, while S-BNC/PVA composite tube possessed a wall thickness of 1.00 ± 0.04 mm. This indicates the external side of S-BNC/PVA composite tube was probably only composed by PVA and water for the reason that the S-BNC tube has thinner wall thickness. Therefore similar morphology of S-BNC/PVA tube with that of PVA tube can be observed. Although the spaces for the culture of BNC tubes of the two bioreactors were same, the double-silicone-tube bioreactor performed higher production efficiency¹³, which led to the wall thickness of D-BNC tube was about 2 times thicker than that of S-BNC tube. Composite tubes made by the tubular mould are identical in wall thickness. Although the original wall thickness of D-BNC tube was 1.27 mm before compositing, the wall thickness of D-BNC/PVA tube was limited to 1 mm in the mould. The wall thickness of PVA tube was 0.89 mm, less than 1 mm (about 10% thinner), which should be ascribed to phase separation process during freezing and thawing.

Table 1 Wall thickness and water permeability of the tubes

PVA tube, BNC tubes and BNC/PVA composite tubes were all hydrogel-like tubes. However the water contents of these hydrogel-like tubes were different for the reason of different components. As shown in Fig. 4, S-BNC tube and D-BNC tube were composed of about 99.7% water and 0.3% BNC. No significant difference in components was detected ($P > 0.05$). The result indicates that both BNC tubes had identical water holding capacity. PVA tube contained about 89.2% water and 10.8% PVA. Obviously BNC tubes performed better water uptake ability, which may be determined by the ultrafine nano-fiber network and more hydrophilic functional group (-OH) in bacterial nano-cellulose. Compared with S-BNC/PVA composite tube, D-BNC/PVA composite tube possessed more BNC content (about 0.87% compared with $0.40 \pm 0.01\%$, $P < 0.05$), which resulted in more water content ($91.5 \pm 1.0\%$ compared with

$90.2 \pm 0.6\%$). The water content was lower than pure BNC tubes, but slightly higher than PVA tube ($P < 0.05$). However PVA in S-BNC/PVA composite tube was much more ($9.40 \pm 0.02\%$ compared with $7.63 \pm 0.01\%$ of D-BNC/PVA tube, $P < 0.05$), which may be related to the more space and multilayered structure, as shown in Fig. 2.

Fig. 4 Composition of PVA tube (a), S-BNC tube (b), D-BNC tube (c), S-BNC/PVA composite tube (d) and D-BNC/PVA composite tube (e). Significant difference between groups is indicated (* $p < 0.05$).

Water permeability

Water permeability is an important performance for artificial blood vessels and grafts. A proper water permeability of small-caliber artificial blood vessel may benefit the endothelialization of the lumen surface since it reflects the permeability of water and transport capacity of nutrients. As reported by Yanguchi et al., water permeability between 10 and $40 \text{ mL} \cdot \text{cm}^{-2} \cdot \text{min}^{-1}$ are positive for the patency rates of artificial vessels³⁴. However, the clinically used ePTFE vessel of 4 mm only possessed a water permeability of $0.43 \text{ mL} \cdot \text{cm}^{-2} \cdot \text{min}^{-1}$ ³⁵. For BNC tubes, the nano-fibers locked a large amount of water in their ultrafine networks. However about 10% water were not held by the BNC molecules, which caused water leakage under the testing condition of water permeability as reported previously³⁶. As illustrated in Tab. 1, the water permeability of S-BNC tube and D-BNC tube were about 3.33 and $2.34 \text{ mL} \cdot \text{cm}^{-2} \cdot \text{min}^{-1}$, respectively, which means good anti-leakage property. The higher water permeability of S-BNC tube might be ascribed to the looser fibre network of external surface and the multi-layered structure as mentioned above. For the clinically used hydrophobic ePTFE and PET vessels, higher water permeability normally means better nutrition transmission to a certain extent, which may benefit cells. On the contrary, for the hydrogel BNC tubes, the large amount water locked in the ultrafine fiber network has provided a good transport environment for nutrition. So the water permeability values here are acceptable. Unfortunately, for PVA tube, the burst pressure was too weak to sustain the testing pressure and broke quickly. For BNC/PVA composite tubes, since PVA molecular interpenetrated into the network of the BNC tubes to form denser composite tubes and sealed the original small pores in the BNC tubes, water leakage should be avoided. As a result, no water leakage was detected under the testing condition. Since PVA tube itself could not tolerate the water pressure, the excellent performance of BNC/PVA tubes indicates that the generated composites had better mechanical strength, which can be attributed to the reinforcement effect from the BNC network.

Mechanical properties

Axial stretch mechanical properties The axial stretch mechanical properties of BNC tubes and BNC/PVA composite tubes are illustrated in Fig. 5. The results showed that D-BNC tube performed higher Young's modulus, tensile strength and elongation at break than S-BNC tube. This is in accordance with the fact that D-BNC tube had thicker fibers and a denser nano-fiber network. As reported previously, the multi-layered structure of S-BNC tube may cause negative effects to the stretch mechanical property³⁷. PVA

tube performed the biggest elongation at break ($162.0 \pm 13.1\%$) ($P < 0.05$), the smallest Young's modulus (0.063 ± 0.009 MPa) ($P < 0.05$) and tensile strength (0.073 ± 0.003 MPa) ($P < 0.05$), but no significant difference in tensile strength was detected as compared with S-BNC tube ($P > 0.05$). The results indicate that PVA tube obtained good ductility and elasticity, but relatively weaker axial stretch mechanical property as compared to the PVA hydrogel tube prepared by a physical crosslinking method, multi freeze-thaw cycles (performed nonlinear mechanical properties similar as cardiovascular tissues)³⁸ for cardiovascular applications. Compared with the performances of PVA tube and BNC tubes, both D-BNC/PVA and S-BNC/PVA composite tubes showed stronger axial stretch mechanical properties. The elongation at break of S-BNC/PVA composite tube was about 39.1%, which is one time bigger than that of S-BNC tube ($20.0 \pm 0.3\%$) ($P < 0.05$). The increase of elongation at break demonstrates the reinforcement effect of PVA. However, the elongation of D-BNC/PVA composite tube and D-BNC tube were $23.1 \pm 1.9\%$ and $24.7 \pm 0.3\%$, respectively. No significant difference before and after the compositing was detected for the D-BNC tube ($P > 0.05$), which illustrates that D-BNC still played determined function (binding effect) on the elongation at break.

Fig. 5 Axial stretch mechanical properties of PVA tube (a), S-BNC tube (b), D-BNC tube (c), S-BNC/PVA composite tube (d) and D-BNC/PVA composite tube (e). Significant difference between groups is indicated (* $p < 0.05$).

For tensile strength, D-BNC/PVA composite tube increased about 131.2% than D-BNC tube (0.19 ± 0.01 MPa) to about 0.45 MPa ($P < 0.05$), while S-BNC/PVA composite tube rose only 83.1% than S-BNC tube (0.09 ± 0.01 MPa) to about 0.17 MPa ($P < 0.05$). The difference reveals the tensile strength of BNC/PVA composite tubes was greatly affected by the base material of BNC. As displayed Young's modulus in Fig. 5, BNC/PVA composite tubes were stiffer than the corresponding BNC tubes and the PVA tube. This should be due to the contribution of a concrete-like structure formed. Similar as the performance of the BNC tubes, D-BNC/PVA composite tube performed higher Young's modulus than S-BNC/PVA tube. Actually it was the biggest value among all the tubes. The S-BNC tube showed looser fiber network and multilayered structure (Fig. 2), which may provide more space for the penetration of PVA, but had the lower BNC content of $0.40 \pm 0.01\%$ compared to D-BNC/PVA composite tube of $0.88 \pm 0.05\%$ ($P < 0.05$) (Fig. 4), illustrating that the BNC nano-fiber network of S-BNC tube may perform weaker constraint to PVA and less reinforcement from BNC network. Therefore S-BNC/PVA composite tube performed better than D-BNC/PVA tube on the elongation at break, but worse on tensile strength and Young's modulus than D-BNC/PVA composite tube. However, compared with the PVA-BNC nanocomposite made by adding PVA powder into BNC suspension solution followed by physical crosslinking, as reported by Millon et al.²⁹, both S-BNC/PVA and D-BNC/PVA composite tube performed stronger Young's modulus because the intact innate ultrafine nano-fiber network of pristine BNC tube were maintained as a skeleton here. When compared with the tensile strength (1.40 - 11.14 MPa) and elongation (45 - 99%) of human coronary artery³⁹, the

mechanical properties of BNC tubes and BNC/PVA tubes were still not comparable to nature vascular tissue. However, the mechanical properties of BNC/PVA tubes can be improved by a following low temperature thermal cycling process, which will be introduced in another article.

Suture retention It is reported that the patency rate of artificial blood vessel after implantation is affected by the suture technique of anastomotic stoma in some degree⁴⁰. A proper suture retention strength may provide more choices for better suture technique. Unfortunately, as shown in Fig. 6, the hydrogel-like PVA tube and the S-BNC tube possessed very poor suture retention strength of about 0.16 N and 0.17 N, respectively. Compared with the suture retention strength of 4.6 ± 0.4 N of the BNC tube made by Scherner et al.⁴¹, the strength values in this study were all somewhat low since the tubes contained too much water (higher than 85%). The difference might depend on less BNC content in the BNC tubes (about 0.3% compared with 1%) and different network density that will vary much because of bacterial strain used and different culture conditions. However, the suture retention strength of the D-BNC tubes (0.37 N) is comparable to the reported values of fresh human tissue-engineered vessels (47 g, namely 0.46 N)⁴². The higher suture retention of D-BNC tubes may be attributed to the bigger wall thickness and the non-layered structure of cross section. After compositing with PVA, the suture retention strength increased to about 0.38 N for S-BNC tube. Similarly, the suture retention strength of D-BNC/PVA composite tube rose from 0.37 N of D-BNC tube to about 0.50 N. Therefore the suture retention strength of the composite tubes may be benefited from both BNC and PVA materials. Although the performance of BNC tubes and BNC/PVA tubes is weaker when compared with the reported suture retention strength of human saphenous vein (1.81 ± 0.02 N) and human mammary artery (1.40 ± 0.01 N)⁴³, it is acceptable for the surgical operation with the manner as reported by Dr. Paul Gatenholm and Dr. Dieter Klemm⁵. Furthermore, the improved stiffness and ductility of BNC/PVA composite tubes makes the suture operation easier.

Fig. 6 Comparison of the suture retention strength of PVA tube (a), S-BNC tube (b), D-BNC tube (c), S-BNC/PVA composite tube (d) and D-BNC/PVA composite tube (e). Significant difference between groups is indicated (* $p < 0.05$).

Burst pressure Fig. 7 illustrates the burst pressures of BNC tubes, PVA tube and BNC/PVA composite tubes. The burst pressures of D-BNC tube and S-BNC tube showed no significant difference (0.028 ± 0.006 MPa and 0.029 ± 0.005 MPa) ($P > 0.05$). The values were corresponding to the BNC tube made by Bodin et al. (250 mmHg, namely 0.033 MPa) with an oxygen ratio over the atmospheric ratio during cultivation³⁷. For burst strength test, BNC tubes always broke at the weakest position. That means the weakest position of D-BNC tube and S-BNC tube had similar burst strength but both pristine BNC tubes can tolerate the normal blood pressure of human body (0.012 - 0.019 MPa, 90-140 mmHg⁴⁴). PVA tube broke at pressure of about 0.0013 MPa, which means it cannot tolerate the normal blood pressure. The result is corresponding to

the weakest axial stretch strength and suture retention. For S-BNC/PVA and D-BNC/PVA composite tubes, the burst strength was improved dramatically to about 0.047 MPa and 0.065 MPa, respectively. BNC fiber network impregnated with PVA may reinforce the burst strength of the vulnerabilities existing in the BNC tubes. The fiber network may restrict the expansion of PVA, which is positive to the improvement of burst pressure.

Fig. 7 Burst pressure of PVA tube (a), S-BNC tube (b), D-BNC tube (c), S-BNC/PVA composite tube (d) and D-BNC/PVA composite tube (e). Significant difference between groups is indicated (* $p < 0.05$).

Circumferential dynamic compliance Compliance mismatch of blood vessel prosthesis to native tissue has been confirmed to be the main reason for the failure of application^{17,45,49}. Fig. 8 shows the circumferential dynamic compliance of PVA tube, BNC tubes and BNC/PVA tubes under pressure of 50-90 mmHg, 80-120 mmHg and 110-150 mmHg. For both BNC tubes, dynamic compliance showed similar results. The mean values of S-BNC tube and D-BNC tube under the test pressure of 80-120 mmHg were biggest to about 3.4% and 3.8%, respectively, which are about two times lower than human arteries⁴⁶, and somewhat higher than that reported for ePTFE (1.92%) and Dacron (1.65%)^{47,48}. While their mean value tested under pressure of 110-150 were smallest to about 1.2% and 2.3%, respectively. The results indicate that under high pressure, the nano-fibers which were entangled in the BNC tube wall might perform stronger restriction to the caliber changes with pressure variation. PVA tube possessed the highest compliance under the three pressure ranges to about 10.7%, 11.7% and 12.2%, respectively. The bigger test pressure was, the bigger compliance obtained, which indicates the weak intermolecular forces among the PVA molecules. Compliance of S-BNC/PVA composite tube under the three pressure ranges showed the same tendency as PVA tube, which was 2.2%, 2.4% and 2.6%, respectively. While that of D-BNC/PVA composite showed adverse tendency, which was 5.6%, 4.9% and 1.9%, respectively. The D-BNC/PVA composite tube performed bigger compliance than the S-BNC/PVA composite tube under the pressure of 50-90 mmHg and 80-120 mmHg, however, much smaller compliance was showed under pressure of 110-150 mmHg. This result might be caused by the more BNC content in D-BNC/PVA composite tube. For human saphenous vein, the compliance is about 0.7-1.5% under the pressure change from 80 to 120 mmHg⁴⁶. Current compliance of the D-BNC/PVA composite tube seems too big, and the S-BNC/PVA composite tube seems to be a suitable candidate. D-BNC/PVA composite tube performed a compliance of $4.9 \pm 0.4\%$ under pressure of 80-120 mmHg, which is accordant with that of human artery ($4.5-6.2\%$)⁴⁶.

Fig. 8 Circumferential dynamic compliance of S-BNC tube (■), D-BNC tube (■), S-BNC/PVA tube (■), D-BNC/PVA tube (■) and PVA tube (■). Significant difference between groups is indicated (* $p < 0.05$).

Cytotoxicity assay

Fig. 9 illustrates continuous proliferation of pig iliac endothelium cells (PIECs) on coverslips, BNC tubes, BNC/PVA composite tubes

and PVA tube at 1, 3, 5 and 7 days after cell seeding, which indicates all samples may support the growth of cells without toxic effects. At day 1, number of viable cells on all samples detected by MTT assay showed no significant difference, but were less than that on coverslips. After day 1, growth of cells performed differently on various materials. For BNC tubes, PIECs proliferated better on the inner surface of S-BNC tube than on that of D-BNC tube. And on the inner surface of PVA tube, PIECs proliferated similar with S-BNC tube. For composite tubes, both S-BNC/PVA and D-BNC/PVA composite tubes performed better proliferation of PIECs compared with the corresponding BNC tubes, which means more suitable for cell growth. Between the two composite tubes, no significant difference in PIECs proliferation was detected in all days.

Fig. 9 Proliferation of PIECs on coverslips, BNC tubes, BNC/PVA composite tubes and PVA tubes at 1, 3, 5 and 7 days after cell seeding. Significant difference between groups is indicated (* $p < 0.05$).

Experimental

Materials

Unless otherwise stated, all chemicals used were analytically pure (Sinopharm Chemical, Shanghai, China) including Poly(vinyl alcohol) ($n=1750 \pm 50$) and ethanol. Dulbecco's Modified Eagle's Medium (DMEM), fetal bovine serum (FBS), 3-(4,5-dimethylthiazol-2-yl)-2,5-diphenyltetrazoliumbromide (MTT), trypsin, penicillin (100 U/mL), and streptomycin (100 $\mu\text{g/mL}$) were supplied by Shanghai Yuanxiang medical equipment CO., Ltd. Pig iliac endothelium cells (PIECs) were purchased from Institute of Biochemistry and Cell Biology (the Chinese academy of Sciences, Shanghai, China).

Strain, culture media and growth conditions

A *Gluconacetobacter xylinus* strain obtained from Hainan Yeguo Foods Co., Ltd., was used as a model strain in the production of bacterial nano-cellulose tubes and maintained on a slant culture medium at 4 °C. The culture medium contained 50 g/L D-glucose, 5 g/L yeast extract (Oxoid), 5 g/L tryptone, 1 g/L citric acid, 1 g/L KH_2PO_4 and 2 g/L Na_2HPO_4 , and initial pH was 5.0.

Preparation of BNC tubes

Two tubular bioreactors were used for the production of BNC tubes. The tubes obtained from the first bioreactor which was assembled with an about 60 mm silicone tube (inner diameter \times external diameter: 2×3 mm) and a glass tube (8×10 mm), similarly as described by Bodin et al.³³, were named as S-BNC tubes. The other bioreactor was composed of two silicone tubes with different calibers (2×3 mm, 8×9 mm), which has been reported by Hong et al.¹³⁻¹⁵. Tubes produced by the latter bioreactor were named as D-BNC tubes.

Two loops of the *G. xylinus* strain were transferred from the agar medium into a 100 mL autoclaved liquid medium and cultivated at 30 °C and 160 rpm on a rotary shaker for 24 h. After agitating cultivation, 20 mL of the seed suspension was inoculated into 180 mL fermentation medium in a 500 mL Erlenmeyer flask. Then, the inoculated flask was maintained at 30 °C and 160 rpm on

a rotary shaker for 4 h. After that, 10 mL of the culture was injected into the tubular bioreactors. The tubular bioreactors were incubated statically at 30 °C for 10 days with the oxygen exchange frequency of once a day.

Purification of BNC tubes

The harvested BNC tubes were rinsed with deionized (D.I.) water several times to remove soluble medium components, followed by treatment with 1% (w/v) sodium hydroxide solution for 4 h at 80 °C to eliminate impurities. After that, the BNC tubes were further purified by boiling in ultrapure water for 2 h. Finally, the hydrogel tubes were rinsed with ultrapure water until pH value was neutral. Thereafter they were stored in ultrapure water at 4 °C.

Preparation of BNC/PVA composite tubes

PVA was first dissolved in 95 °C ultrapure water, which was incubated in a shaking water bath machine with a rate of 100 rpm, then 95% ethanol was added into the aqueous solution to form homogeneous solution containing 10% (w/v) PVA and 20% (v/v) ethanol. The homogeneous solution was cooled to room temperature for further use.

A BNC hydrogel tube with size of 50 mm in length and 3 mm in inner diameter covered on a glass rod with a diameter of 3 mm. About 95% water in the hydrogel tube was removed slowly with filter paper. Then the tube with glass rod was inserted into a polypropylene tube with internal diameter of 5 mm and external diameter of 7 mm to form a tubular mould for the preparation of BNC/PVA composite hydrogel tube. The PVA solution prepared above was then injected into the cavity between the polypropylene tube and the glass rod. After that the tubular mould was put at room temperature for 24 h to let the BNC tube swell adequately in the PVA solution. Then it was placed at -80 °C for 4 h followed by thawing in cold anhydrous ethanol (-20 °C) for 24 h, before thawing the seal rings at the ends of the mould tube were removed. The composite tube was then taken out from the mould tube and was immersed into ultrapure water at room temperature to exchange alcohol for 3 days. The water was changed every 4 h. Finally, the obtained BNC/PVA composite tube was stored in ultrapure water at 4 °C. For the preparation of PVA tube, the same procedure was followed as described above for the preparation of BNC/PVA composite tube except that a glass rod with a diameter of 3 mm was directly inserted into a polypropylene tube with internal diameter of 5 mm and external diameter of 7 mm to form a tubular mould.

Characterizations

For macro-morphology analysis, pictures of all tubes were taken by the (CMOS) camera of an automatic colony counter (Shineso, Hangzhou, China). All tubes were cut off a small part and immersed in water in a glass plate. The external and sectional view of all tubes was then taken by the camera.

For scanning electron microscope (SEM) analysis, samples were freeze-dried first and were coated with a thin layer of evaporated gold, and images were taken using a JSM-5600LV scanning electron microscope (JEOL, Japan) with an acceleration voltage of 15 KV. In order to determine average diameters size and

fiber distribution of the BNC tubes, more than 100 fibers were randomly selected from the SEM images and the diameter was measured by using an image analysis software Image-J (NIH, USA).

Wall thicknesses of tubes were measured by a digital caliper. Tubes were first immersed in ultrapure water for three days to swelling equilibrium. Wall thickness of every tube was obtained from the mean value of at least five samples.

Water permeability was tested following the method described in ISO 7198:1998(E) standard. Briefly, a reservoir was connected to a polypropylene tube followed by the sample. An intraluminal pressure of 0.16 MPa hydrostatic pressure was applied into the sample. The permeated water through the tube wall per minute was collected and calculated in mL cm⁻² min⁻¹.

Tensile evaluation was performed on a universal material testing machine (H5K-S, Hounsfield, UK) under ambient condition (room temperature, around 50% relative humidity) at a speed of 10 mm min⁻¹ with a 10 N sensor loaded. The mean value was obtained from at least five tubular samples with the size of 5 cm in length.

Suture retention was detected by the universal material testing machine mentioned above. Samples were cut with length of 20 mm. A single 2-mm bite of 5-0 Dacron suture with BV-1 needle was placed at the end of the cut and pulled out at a rate of 50 mm/min until failure. The mean value was obtained from at least five tubular samples.

For determination of water content, the tubes were stored in ultrapure water for at least three days, and then were sponged by filter papers to remove the water on the surface and immediately weighed to record the weight of wet tubes (W_{wet}). After dehydrating samples at 105 °C for 12 h, the weight of dry tubes (W_{dry}) was measured. The water content (WC) of the tubes was calculated as follows:

$$\text{WC} = \frac{(W_{\text{wet}} - W_{\text{dry}})}{W_{\text{wet}}} \times 100\%$$

Cellulose content of BNC/PVA tubes was calculated as follows:

$$\text{CC} = \frac{L \times W_{\text{bnc}}}{W_{\text{wet}}} \times 100\%$$

where: W_{bnc} and L are the dry weight of per meter BNC tubes and the exact length of BNC/PVA composite tubes, respectively. W_{wet} is the weight of each wet tube.

Burst pressure was tested by using a home-made equipment, which was assembled with a pressure gage and an injector. Tubular sample with a size of 40 mm in length was well connected to the equipment. Water was injected into the tube with a speed of 0.01 MPa/s. The pressure in the tube was kept for 10 s at every 0.02 MPa. The pressure at the point of the sudden broken of the tube was recorded as the burst pressure.

Dynamic compliance at the circumferential direction was tested by BOSE BioDynamic test machine (Bose, USA) following the method described in ISO 7198:1998(E). The diameter change of the tube accompanied with the pressure variation between 50-90 mmHg, 80-120 mmHg and 110-150 mmHg was recorded respectively. The compliance was calculated as follow:

$$\text{Compliance (\%)} = \frac{(R_{P_2} - R_{P_1})/R_P}{P_2 - P_1} \times 10^4$$

where: P_1 is the lower pressure value, in mmHg; P_2 is the higher pressure value, in mmHg; R_p is the pressurized internal radius, in mm⁴⁹.

For cytotoxicity assay, PIECs were cultured in a 5% CO₂, humid atmosphere at 37 °C in DMEM medium supplemented with 10% FBS, 100 U mL⁻¹ penicillin and 100 µg mL⁻¹ streptomycin. Briefly, tubular samples were longitudinally cut with a size about 15 mm in length and 9 mm in width. Then the samples were sterilized in 75% ethanol for 12 h, followed by washing with PBS buffer to eliminate alcohol under sterile condition. After that, the samples were fixed at the well bottom of 24-well plate with stainless steel rings to make the inner surface upward. Cell culture medium of 400 µL was added into each well to pretreat the samples for 12 h. PIECs were then seeded onto the samples with cell density of 1×10⁴ cells per well and cultured. MTT assay was taken at culture time of 1, 3, 5, and 7 days, respectively, and coverslip was served as a control. The seeded samples were washed three times with PBS in the plates. Then 360 µL DMEM and 40 µL MTT was added into every well. After incubation at 37 °C with 5% CO₂ for 4 h, the solution was carefully removed and 400 µL dimethyl sulfoxide was added. After being shaken at 100 rpm and 37 °C for 30 min, 100 µL solution was transferred into 96-well culture plate and measured at 492 nm by microplate reader (Multiskan MK3, Thermo Labsystems, China)⁵⁰.

Conclusions

Two kinds of BNC tubes and their corresponding composite tubes doped with PVA were prepared and evaluated for potential applications in artificial blood vessel. Results revealed pristine BNC tubes showed some insufficient properties for vascular grafts, such as poor suture retention and water leakage. Through compositing BNC with PVA the mechanical properties and water permeability were improved dramatically compared to PVA tube and BNC tubes. In the composite tubes, BNC tubes determined the final mechanic properties as basic materials. The S-BNC/PVA composite tube possessed weaker mechanical properties than D-BNC/PVA composite tube, which might be more suitable for veins. The D-BNC/PVA composite tube with better compliance demonstrated great potential for artery transplantation. However more works like more detailed biocompatibility studies and animal experiments are needed in further investigation.

Acknowledgements

Sponsoring funds: Financial supports provided by Program for New Century Excellent Talents in University (NCET-12-0828), by the National Natural Science Foundation of China (No. 51373031), the Science and Technology Commission of Shanghai Municipality (12nm0500600), the 111 Project B07024, and the Fundamental Research Funds for the Central Universities (2232014A3-04) are gratefully acknowledged.

References

- 1 D. G. Seifu, A. Purnama, K. Mequanint and D. Mantovani, *Nat. Rev. Cardiol.* 2013, 10, 410-421.
- 2 O. E. Teebken and A. Haverich, *Eur. J. Vasc. Endovasc. Surg.* 2002, 23, 475-485.
- 3 R. D. Sayers, S. Raptis, M. Berce and J. H. Miller, *Br. J. Surg.* 1998, 85, 934-938.
- 4 D. A. Schumann, J. Wippermann, D. O. Klemm, F. Kramer, D. Koth, H. Kosmehl, T. Wahlers and S. Salehi-Gelani, *Cellulose* 2008, 16, 877-885.
- 5 P. Gatenholm and D. Klemm, *MRS Bull.* 2010, 35, 208-213.
- 6 A. Putra, A. Kakugo, H. Furukawa, J. P. Gong and Y. Osada, *Polymer* 2008, 49, 1885-1891.
- 7 N. Petersen and P. Gatenholm, *Appl. Microbiol. Biotechnol.* 2011, 91, 1277-1286.
- 8 H. Fink, J. Hong, K. Drotz, B. Risberg, J. Sanchez and A. Sellborn, *J. Biomed. Mater. Res. A* 2011, 97A, 52-58.
- 9 M. Rouabhia, J. Asselin, N. Tazi, Y. Messaddeq, D. Levinson and Z. Zhang, *ACS Appl. Mater. Interfaces* 2014, 6 (3), 1439-1446.
- 10 H. Bäckdahl, G. Helenius, A. Bodin, U. Nannmark, B. R. Johansson, B. Risberg and P. Gatenholm, *Biomaterials* 2006, 27, 2141-2149.
- 11 D. Klemm, D. Schumann, U. Udhardt and S. Marsch, *Prog. Polym. Sci.* 2001, 26, 1561-1603.
- 12 J. Wippermann, D. Schumann, D. Klemm, H. Kosmehl, S. Salehi-Gelani and T. Wahlers, *Eur. J. Vasc. Endovasc. Surg.* 2009, 37, 592-596.
- 13 F. Hong, B. Wei and L. Chen, *BioMed. Res. Int.* 2015, Article ID 560365, 9 pages, doi:10.1155/2015/560365 (www.hindawi.com/journals/bmri/aa/560365/).
- 14 F. Hong, B. Wei, and G. Yang, Device for preparing hollow specially-shaped bacterial cellulose material, *China Pat.* 2010, CN201809341/CN20102511755U, 2010-09-02, <http://worldwide.espacenet.com/>.
- 15 F. Hong, B. Wei, and G. Yang, Device and method for preparing hollow heteromorphic bacteria cellulose material, *China Pat.* 2010, CN101921700/CN20101270524, 2010-09-02, <http://worldwide.espacenet.com/>.
- 16 R. J. van Det, B. H. R. Vriens, J. van der Palen and R. H. Geelkerken, *Eur. J. Vasc. Endovasc. Surg.* 2009, 37, 457-463.
- 17 H. Prichard, R. Manson, L. DiBernardo, L. Niklason, J. Lawson and S. M. Dahl, *J. Cardiovasc. Transl. Res.* 2011, 4, 674-682.
- 18 Y. Mori, H. Tokura and M. Yoshikawa, *J. Mater. Sci.* 1997, 32, 491-496.
- 19 V. I. Lozinsky and F. M. Plieva, *Enzyme Microb. Technol.* 1998, 23, 227-242.
- 20 W. K. Wan, G. Campbell, Z. F. Zhang, A. J. Hui and D. R. Boughner, *J. Biomed. Mater. Res.* 2002, 63, 854-861.
- 21 J. Wang, C. Gao, Y. Zhang and Y. Wan, *Mater. Sci. Eng. C* 2010, 30, 214-218.
- 22 S. Gea, E. Bilotti, C. T. Reynolds, N. Soykeabkeaw and T. Peijs, *Mater. Lett.* 2010, 64, 901-904.
- 23 Indriyati, R. Yudianti and M. Karina, *Pro. Chem.* 2012, 4, 73-79.
- 24 M. Stroescu, A. Stoica-Guzun and I. M. Jipa, *J. Food Eng.* 2013, 114, 153-157.

- 25 R. D. Pavaloiu, A. Stoica-Guzun, M. Stroescu, S. I. Jinga and T. Dobre, *J. Biol. Macromol.* 2014, 68, 117-124.
- 26 A. Stoica-Guzun, M. Stroescu, I. Jiapa, L. Dobre and T. Zaharescu, *Radiat. Phys. Chem.* 2013, 84, 200-204.
- 27 K. Qiu and A. Netravali, *J. Mater. Sci.* 2012, 47, 6066-6075.
- 28 L. E. Millon, C. J. Oates and W. Wan, *J. Biomed. Mater. Res. B Appl. Biomater.* 2009, 90B, 922-929.
- 29 L. E. Millon and W. K. Wan, *J. Biomed. Mater. Res. B Appl. Biomater.* 2006, 79B, 245-253.
- 30 A. F. Leitão, J. P. Silva, F. Dourado and M. Gama, *Materials* 2013, 6, 1956-1966.
- 31 L. E. Millon, G. Guhados and W. Wan, *J. Biomed. Mater. Res. B Appl. Biomater.* 2008, 86B, 444-452.
- 32 A. F. Leitão, S. Gupta, J. P. Silva, I. Reviakine and M. Gama, *Colloids Surf. B Biointerfaces* 2013, 111, 493-502.
- 33 A. Bodin, H. Bäckdahl, L. Gustafsson, B. Risberg and P. Gatenholm, in *Modern Multidisciplinary Applied Microbiology*, Wiley-VCH Verlag GmbH & Co. KGaA, 2008, pp 619-622.
- 34 T. Yaguchi, A. Funakubo, T. Okoshi, Y. Noishiki and Y. Fukui, *J. Artif. Organs* 2002, 5, 117-122.
- 35 H. Martz, G. Beaudoin, R. Paynter, M. King, D. Marceau and R. Guidoin, *J. Biomed. Mater. Res.* 1987, 21, 399-412.
- 36 K. Gelin, A. Bodin, P. Gatenholm, A. Miharanyan, K. Edwards and M. Strømme, *Polymer* 2007, 48, 7623-7631.
- 37 A. Bodin, H. Bäckdahl, H. Fink, L. Gustafsson, B. Risberg and P. Gatenholm, *Biotechnol. Bioeng.* 2007, 97, 425-434.
- 38 L. E. Millon, H. Mohammadi and W. K. Wan, *J. Biomed. Mater. Res. B Appl. Biomater.* 2006, 79B, 305-311.
- 39 J. Valenta, in *Biomechanics (Clinical aspects of biomedicine)*, ed. J. Valenta, Amsterdam, Elsevier Science Press, 1993, p 142-179.
- 40 X. Kong, B. Han, H. Wang, H. Li, W. Xu and W. Liu, *J. Biomed. Mater. Res. A* 2012, 100A, 1938-1945.
- 41 M. Scherner, S. Reutter, D. Klemm, A. Sterner-Kock, M. Guschlbauer, T. Richter, G. Langebartels, N. Madershahian, T. Wahlers and J. Wippermann, *J. Surg. Res.* 2014, 189, 340-347.
- 42 C. Quint, M. Arief, A. Muto, A. Dardik and L. E. Niklason, *J. Vasc. Surg.* 2012, 55, 790-798.
- 43 G. König, T. N. McAllister, N. Dusserre, S. A. Garrido, C. Iyican, A.; Fiorillo, A. Marini, H. Avila, W. Wystrychowski, K. Zagalski, M. Maruszewski, A. L. Jones, L. Cierpka, L. M. de la Fuente and N. L'Heureux, *Biomaterials* 2009, 30, 1542-1550.
- 44 S. Wang, Y. Zhang, G. Yin, H. Wang and Z. Dong, *J. Appl. Polym. Sci.* 2009, 113, 2675-2682.
- 45 H. Sonoda, S.-I. Urayama, K. Takamizawa, Y. Nakayama, C. Uyama, H. Yasui and T. Matsuda, *J. Biomed. Mater. Res.* 2002, 60, 191-195.
- 46 N. L'Heureux, N. Dusserre, G. König, B. Victor, P. Keire, T. N. Wight, N. A. F. Chronos, A. E. Kyles, C. R. Gregory, G. Hoyt, R. C. Robbins and T. N. McAllister, *Nat. Med.* 2006, 12, 361-365.
- 47 M. Zidi and M. Cheref, *Comput. Biol. Med.* 2003, 33, 65-75.
- 48 A. M. Seifalian, H. J. Salacinski, A. Tiwari, A. Edwards, S. Bowald and G. Hamilton, *Biomaterials* 2003, 24, 2549-2557.
- 49 M. J. McClure, D. G. Simpson and G. L. Bowlin, *J. Mech. Behav. Biomed. Mater.* 2012, 10, 48-61.
- 50 W. Wang, J. Hu, C. He, W. Nie, W. Feng, K. Qiu, X. Zhou, Y. Gao and G. Wang, *J. Biomed. Mater. Res. A* 2015, 103, 1784-1797.

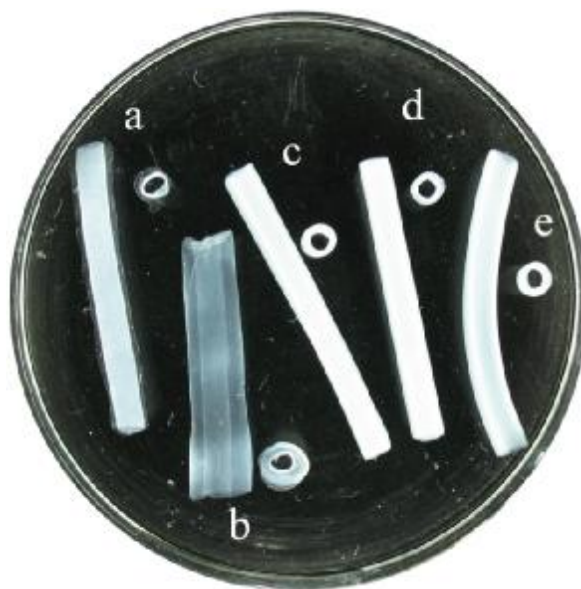


Fig. 1 Macro-morphology of S-BNC tube (a), D-BNC tube (b), S-BNC/PVA composite tube (c), D-BNC/PVA composite tube (d) and PVA tube (e).

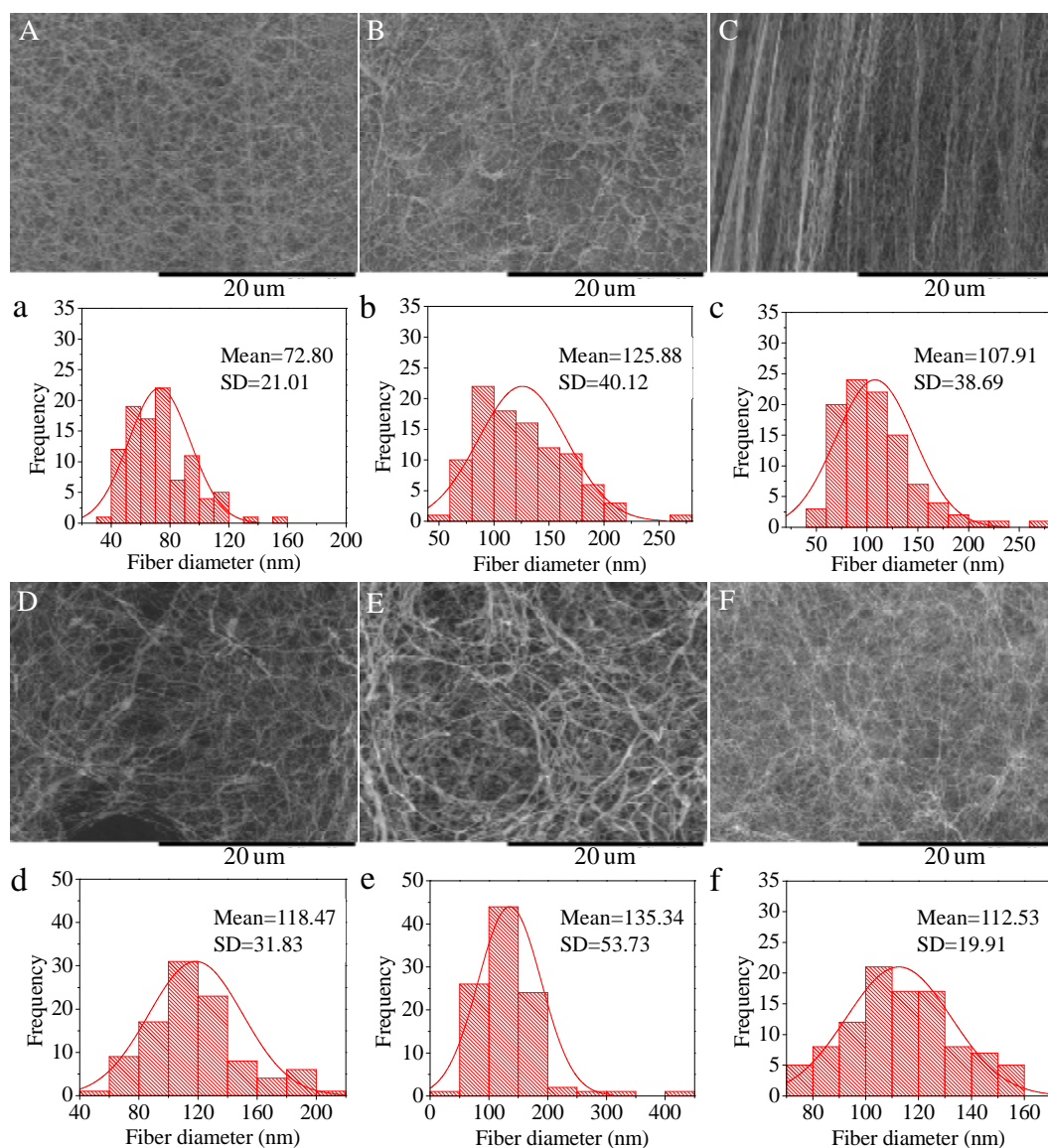


Fig. 2 SEM micrographs and fiber diameter distributions of BNC tubes. SEM images of external surface (A), internal surface (B), and cross section (C) of S-BNC tube, as well as distribution of fiber diameter corresponding to image A (a), B (b), and C (c), are shown respectively. SEM image of external surface (D), internal surface (E), and cross section (F) of D-BNC tube, as well as distribution of fiber diameter corresponding to image D (d), E (e), and F (f), are shown respectively.

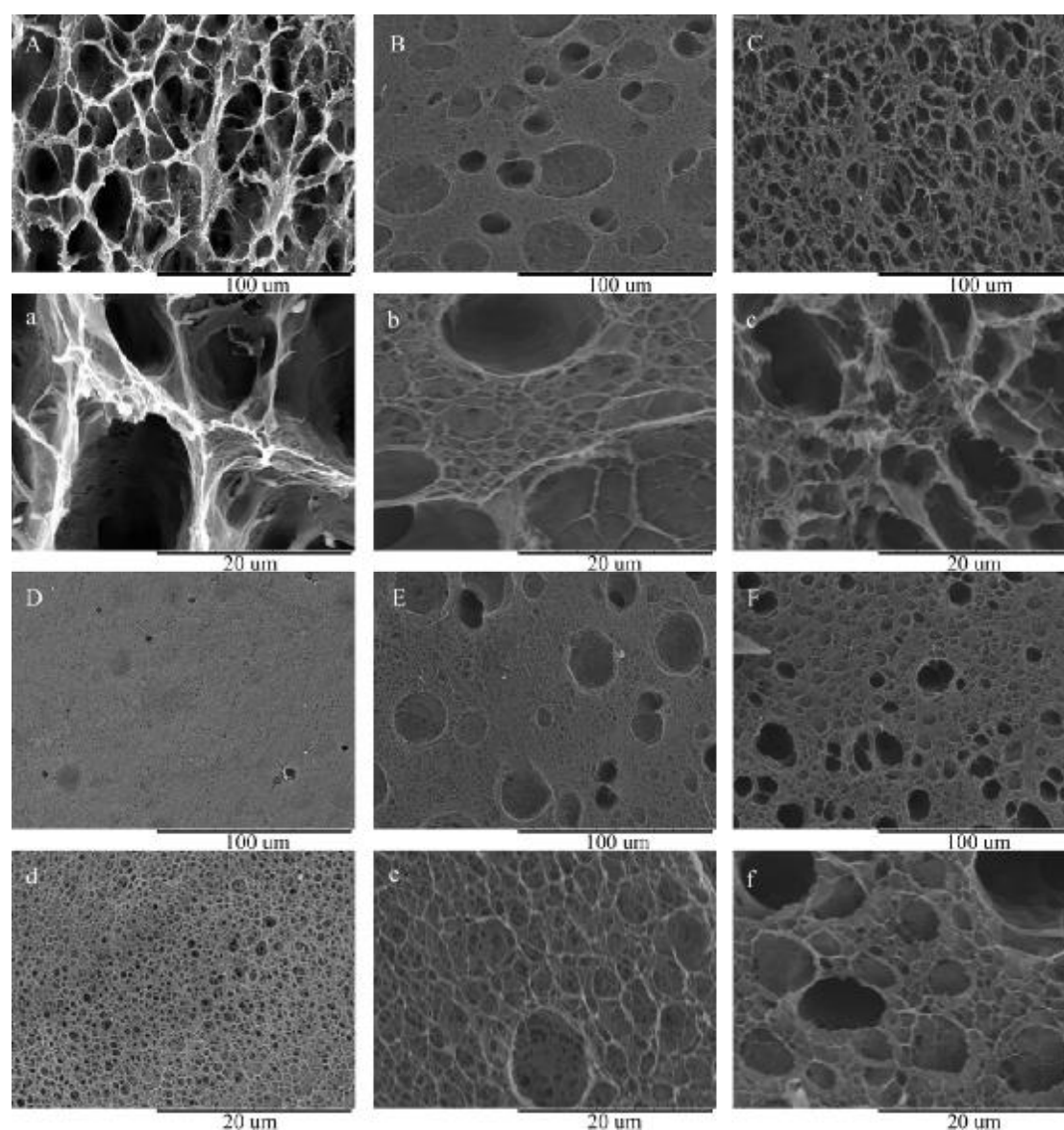


Fig. 3 SEM micrographs of: S-BNC/PVA composite tube, D-BNC/PVA composite tube and PVA tube. The external surfaces of S-BNC/PVA composite tube (A), D-BNC/PVA composite tube (B) and PVA tube (C), as well as the internal surfaces of S-BNC/PVA composite tube (D), D-BNC/PVA composite tube (E), and PVA tube (F) are displayed in amplification of 1000 times, respectively. SEM images of a-f in amplification of 5000 times correspond to the images of A-F.

Table 1 Wall thickness and water permeability of the tubes

Tubes	Wall thickness (mm) [§]	Water permeability (mL·cm ⁻² ·min ⁻¹) ^{§§}
S-BNC tube	0.65±0.11	3.33±0.13
D-BNC tube	1.27±0.10	2.34±0.10
PVA tube	0.89±0.01	Break
S-BNC/PVA tube	1.00±0.04	0 (no leakage)
D-BNC/PVA tube	1.01±0.04	0 (no leakage)

[§]: For wall thickness, significant difference between groups ($p < 0.05$) was found; ^{§§}: For water permeability, significant difference between groups ($p < 0.05$).

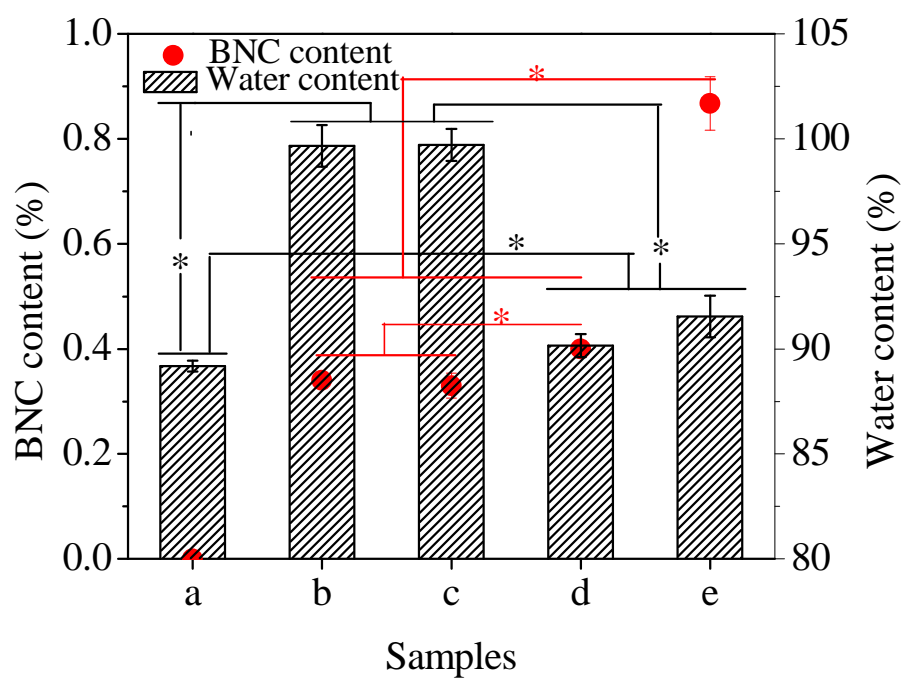


Fig. 4 Composition of PVA tube (a), S-BNC tube (b), D-BNC tube (c), S-BNC/PVA composite tube (d) and D-BNC/PVA composite tube (e). Significant difference between groups is indicated (* $p < 0.05$).

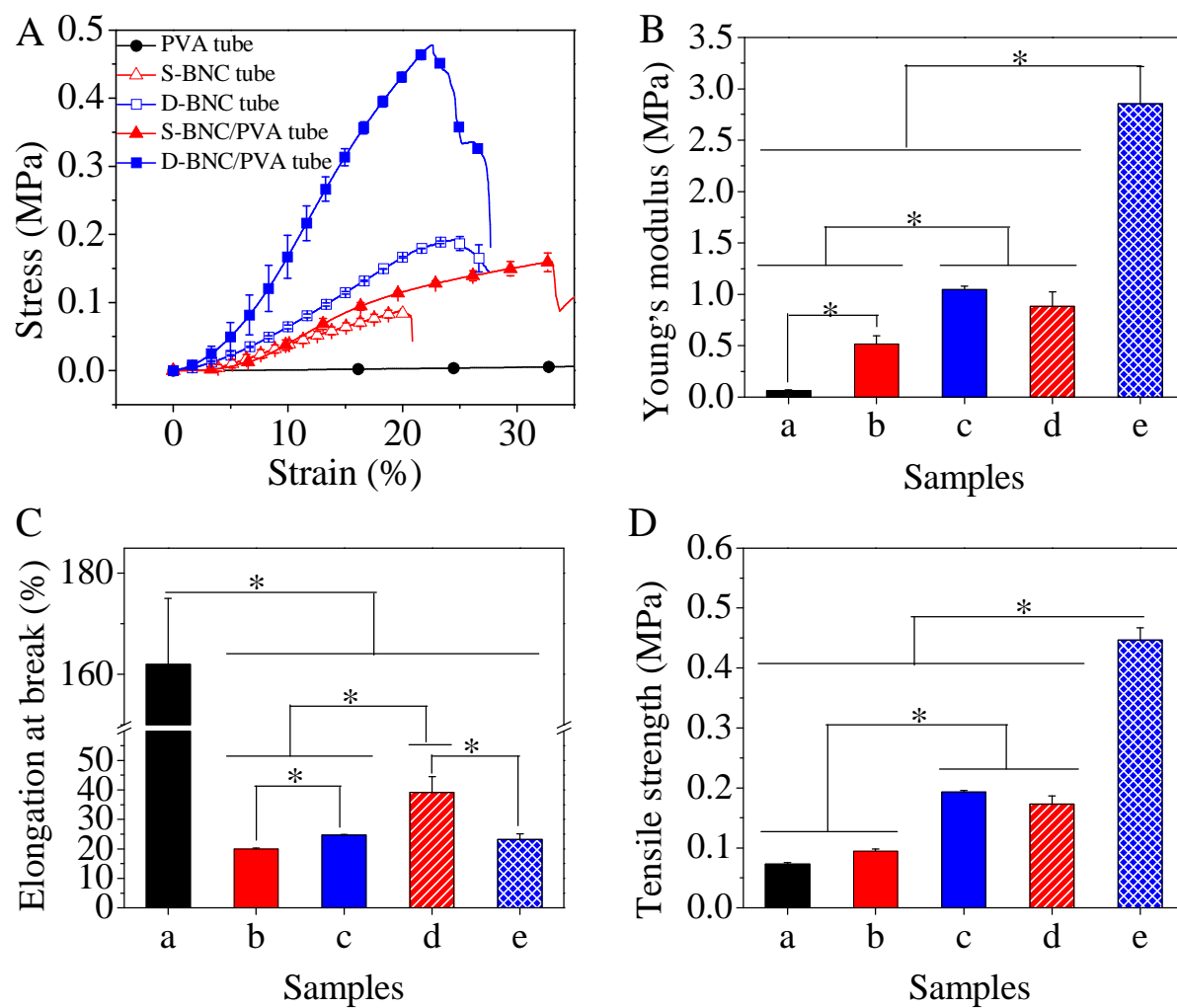


Fig. 5 Axial stretch mechanical properties of PVA tube (a), S-BNC tube (b), D-BNC tube (c), S-BNC/PVA composite tube (d) and D-BNC/PVA composite tube (e). Significant difference between groups is indicated (* $p < 0.05$).

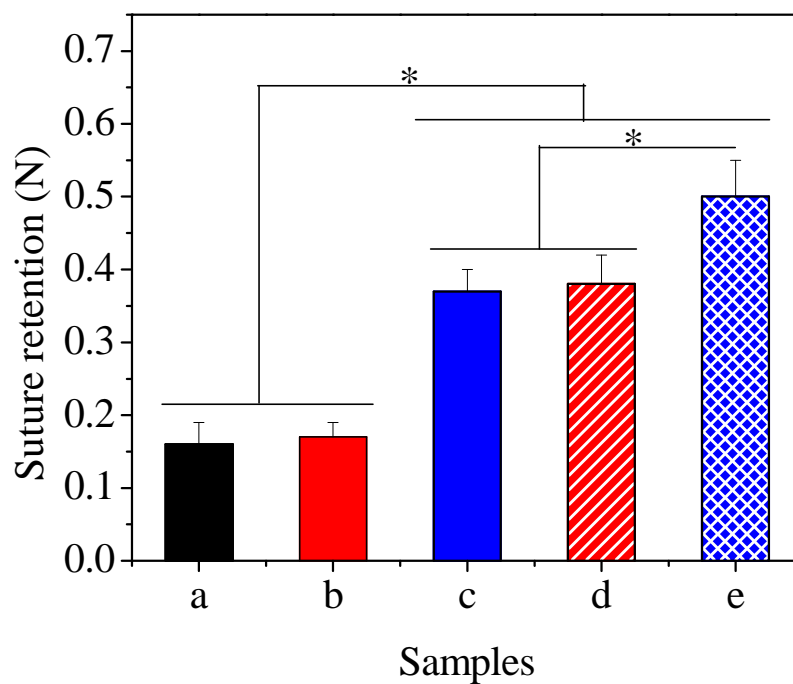


Fig. 6 Comparison of the suture retention strength of PVA tube (a), S-BNC tube (b), D-BNC tube (c), S-BNC/PVA composite tube (d) and D-BNC/PVA composite tube (e). Significant difference between groups is indicated (* $p < 0.05$).

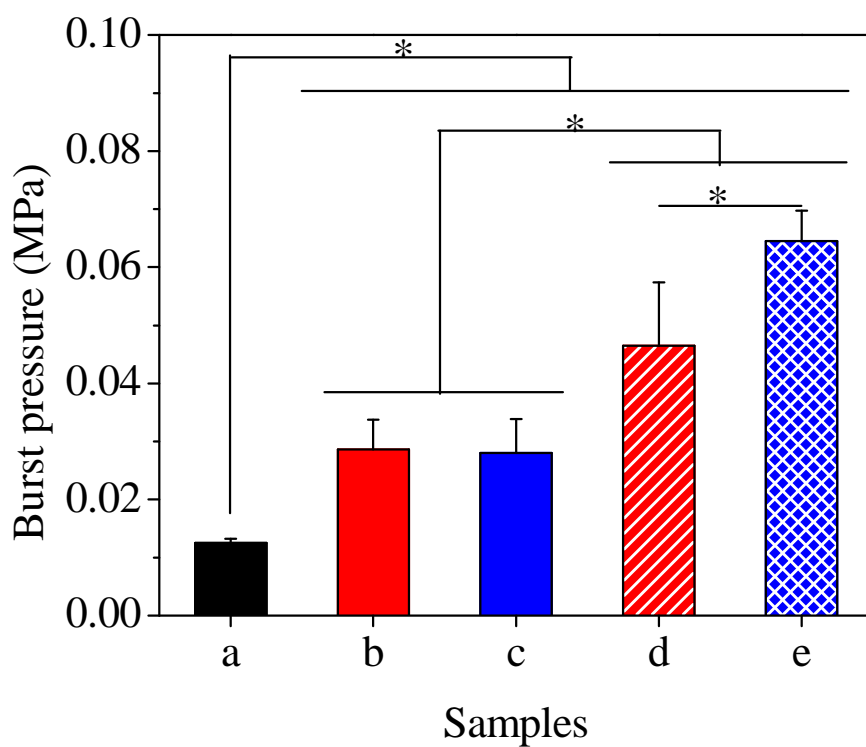


Fig. 7 Burst pressure of PVA tube (a), S-BNC tube (b), D-BNC tube (c), S-BNC/PVA composite tube (d) and D-BNC/PVA composite tube (e). Significant difference between groups is indicated (* $p < 0.05$).

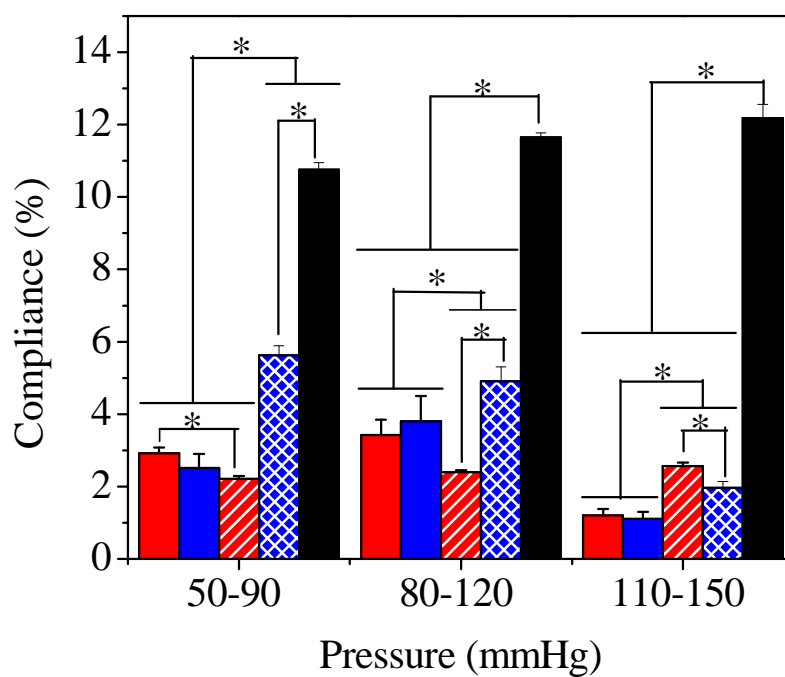


Fig. 8 Circumferential dynamic compliance of S-BNC tube (■), D-BNC tube (■), S-BNC/PVA tube (■), D-BNC/PVA tube (■) and PVA tube (■). Significant difference between groups is indicated (* $p < 0.05$).

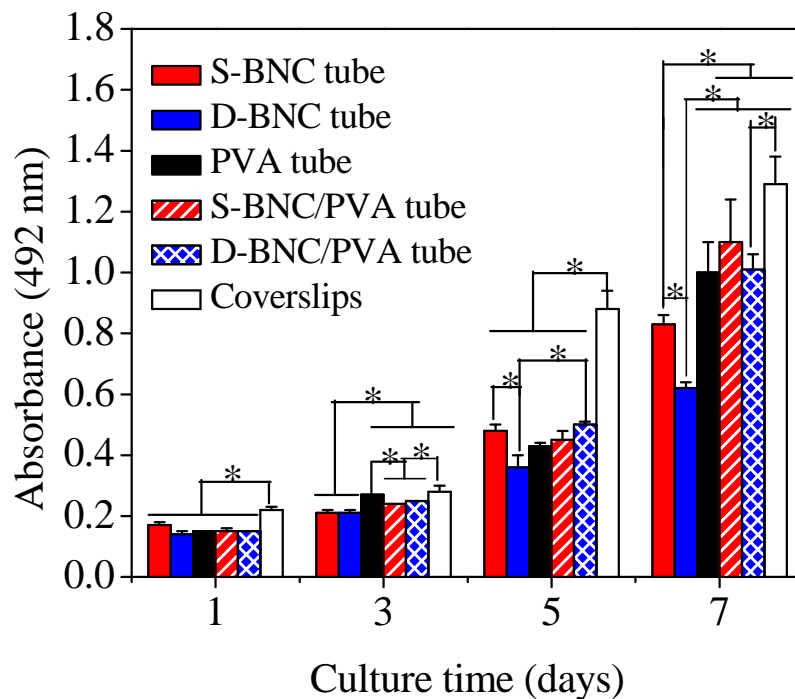


Fig. 9 Proliferation of PIECs on coverslips, BNC tubes, BNC/PVA composite tubes and PVA tubes at 1, 3, 5 and 7 days after cell seeding. Significant difference between groups is indicated (* $p < 0.05$).

Table of Contents/Abstract Graphic

